Embodied Latch Mechanism of the Mandible to Power at an Ultrahigh Speed in the Trap-jaw Ants *Odontomachus kuroiwae*

Hitoshi Aonuma[1*], Keisuke Naniwa[1,+], Yasuhiro Sugimoto[2], Kyohsuke Ohkawara[3], and Katsushi Kagaya[4]

[1]Graduate School of Science, Kobe University, 1-1 Rokkodai, Nada-ku, Kobe, Hyogo 657-8501, Japan

[2] Department of Mechanical Engineering, Osaka University, Suita, Osaka 565-0871, Japan

[3] Division of Biological Sciences, Graduate School of Natural Science and Technology, Kanazawa University, Kanazawa, Ishikawa 920-1192, Japan

[4] Graduate School of Information Science and Technology, The University of Tokyo, 7-3-1 Hongo, Bunkyo-ku, Tokyo 113-8656, Japan

Running title: Latching mechanism of the trap-jaw ant

Figures 7, Table 1

[*]: Address for Correspondence: Hitoshi Aonuma, D.Sc.,

Graduate School of Science, Kobe University, 1-1 Rokkodai, Nada-ku, Kobe, Hyogo 657-8501, Japan

Tel/Fax: +81-78-803-5718, Email: aon@sapphire.kobe-u.ac.jp

[+]: Present address: Department of Mechanical Engineering, Osaka University, Suita, Osaka 565-0871, Japan

Abstract

Quick movements faster than muscle contraction are mediated by a mechanical network of springs and latches. The latch system centers the network operation, but the refined anatomical embodiment remains obscure. The trap-jaw ant *Odontomachus kuroiwae* closes the mandible extremely fast to capture prey and to perform mandible-powered defensive jumps to avoid potential threat. The jump is mediated by mechanical spring and latch systems embodied in the mandible. The ant hits the tip of the mandible on the surface of an obstacle (prey, predator, or ground) to bounce its body. The angular velocity of the closing mandible was 2.3×10^4 rad/s. Latching the joint is one of the most important mechanisms to accumulate the energy and power the mandibles. We identified the fine structure of the latch on the mandible forming a 'ball-joint' using an X-ray micro-computational tomography system (X-ray micro-CT) and X-ray live imaging with a synchrotron. We here highlight a fine projection on the surface of the ball lip and the surface of the inner section of the socket. The height of the projections on the surface of the ball was 3.8±1.8 µm and on the socket was 6.8±2.7 µm. The X-ray live imaging and movement of the 3D model show that the ball with the detent ridge slipped into the socket and over the socket ridge before snapping back at the groove edge. The snapping back movement is quantified in the ultra-fast systems. Our results give an insight into the complex, tightly coupled spring-latch system.

Introduction

Speed is a crucial ingredient for animals to survive in their changing environments. During the prey-predator encounter, either the predator or the prey moves fast; the first to capture the prey and the latter to escape from threat. Evolving power-amplified quick movements is one of the strategies for animals to survive a potential threat and capture elusive prey. Arthropod animals evolved specialized appendages to produce quick movements (e.g. locust; (Heitler, 1974), dragonfly; (Pritchard, 1965), mantis shrimp; (Patek et al., 2004) and snapping shrimp (Ritzmann, 1974; Versluis et al., 2000). The movements over the physiological limit of muscle contraction are controlled by dynamically coupled, neuro-mechanical systems. The locust jump, for example, is one of the quickest movements to escape from the predatory threat which has been well investigated (Burrows, 1995). The locust fully flexes the hindleg to prepare for the jump and co-contracts the extensor and flexor tibia muscles. Then the extensor tibia muscles slowly contract to store energy in the extensor apodeme and exoskeleton. The jump is triggered by the inhibition of motor neurons and flexor muscles. An energy storage before quick movement of the labium is also observed in the dragonfly larva (Tanaka and Hisada, 1980). The extensor and flexor muscles of the labium are co-contracted before quick extension. Relaxation of the flexor muscles and a hydraulic mechanism produce a predatory strike at a high speed (Tanaka and Hisada, 1980). Mantis shrimp store elastic energy at the exoskeleton to generate to power a quick raptorial strike (Zack et al., 2009) where an exoskeletal spring mechanism with several components such as saddle or ventral bar is thought to be a key (Patek et al., 2004).

The ants genus *Odontomachus* have long and powerful mandible so-called

trap-jaw that functions as a weapon when hunting (De la Mora et al., 2008). The ant closes the mandible extremely fast to capture prey (Gronenberg et al., 1993; Gronenberg, 1996; Just and Gronenberg, 1999). Using the mandible, the trap-jaw ant performs the jump so-called bouncer defense (Patek et al., 2006; Spagna et al., 2009). More aggressive ants respond to unexpected tactile stimuli with defensive behavior and potentially show the mandible-powered jump (Aonuma, 2020). The jump is thought to increase survival rate during predator-prey encounters (Larabee and Suarez, 2015). The trap-jaw ants approach prey by fully opening the mandible. The mandible has mechanoreceptive hairs able to detect prey and capture it at an ultra-fast speed. The sensory neurons originated from the hairs innervate into the suboesophageal ganglion to activate mandibular motor neurons (Gronenberg and Tautz, 1994; Gronenberg et al., 1993; Gronenberg, 1995). The key to the ultra-fast movements is thought to be the mechanisms of the power amplification realized by the combination of the catapult mechanism and elastic energy storage in the apodeme and skeletal systems (Gronenberg, 1996). The ultra-fast movement of the mandible consists of 4 phases: (i) open, (ii) latch, (iii) load, and (iv) strike phase. The contraction of the mandible abductor muscles opens the mandible, and the mandible fully opened is latched to prepare for the loading phase. The contraction of the adductor muscles introduces the loading phase, and the contraction of the trigger muscle releases the latch to promote a quick strike of the mandible (Gronenberg and Ehmer, 1996). The latching mechanism is one of the key mechanisms for the trap-jaw ants to power the mandible strike at an ultra-fast speed.

We here performed X-ray micro-imaging to scrutiny fine structure that could function as embodied latch in the mandible joint. X-ray micro-CT scanning and X-ray

in vivo live imaging demonstrate that the mandible joint of the trap-jaw ant genus *Odontomachus* is like ball-joint with fine projections on the surface of the lip and the inner section of the socket.

Materials and Methods

Animals

Workers of the trap-jaw ants *Odontomachus kuroiwae* were mainly used in this study. Colonies of the trap-jaw ants *O. kuroiwae* were collected in Okinawa. The trap-jaw ants *Odontomachus monticola* (Emery 1892) collected in Osaka were also used to compare the performance of striking the mandible. The two species have been classified as different species (Yoshimura et al., 2007). However, since they are closely related, the morphological characteristics are quite similar. The trap-jaw ants are mostly polygynous and contained 3-4 queens, 100-300 of workers and broods. Each colony was installed into an artificial plaster nest (200 mm×200 mm×40 mm) in a plastic case (600 mm×400 mm×200 mm) on a 14:10 hr. light and dark cycle (lights on at 6:00) at 25±2˚C. They were fed a diet consisting of insect jelly (Marukan Co., Ltd, Osaka, Japan), cricket nymphs and water *ad libitum*. Notably, there are no distinctive differences between major and minor workers both in *O. kuroiwae* and *O. monticola*.

Mandible powered defensive jump

The trap-jaw ants genus *Odontomachus* show mandible powered jump named bouncer defense (Patek et al., 2006; Spagna et al., 2009). We first gained the information of the mandible powered jump in another species *O. kuroiwae* and *O. monticola*. A trap-jaw

ant was placed into an acrylic arena (450×450×200 mm). After a short rest (5mim), the mandible-powered jump was introduced by the tactile stimulation using a stick. The trap-jaw ant responded to the approaching stick by turning to the stick and opening the mandible (Aonuma, 2020). Since the mandible has mechanosensory hairs that detect touching an obstacle (Gronenberg et al., 1993), the tactile stimulation was given to the sensory hairs. Mandible powered jumps of the trap-jaw ants were recorded using a pair of high-speed cameras that were placed at the top and one side of the arena (2,000 fps, HAS U2, DITECT, Tokyo, Japan). Each flame was stored as TIFF format for later analysis. The movement of the ant was tracked to measure jump velocity using an open-source video tracking software Kinovea (Ver 0.8.15, https://www.kinovea.org).

Recording ultrafast movements of the mandible

The movement of the mandibles was observed under dissection microscope (SZX-12, Olympus, Tokyo, Japan). A trap-jaw ant was anesthetized using carbon dioxide gas and mounted on a plastic platform using a wax (GC corporation, Tokyo, Japan). Ultrafast movement of the mandibles was elicited by air puff stimulation onto the head and recorded using a high-speed camera (10,000-60,000 fps, HAS D71, DITECT, Tokyo, Japan) attached on the dissection microscope and each flame was stored as TIFF format for later analysis. The movement of the tip of the mandible was tracked to measure the angular velocity using the video tracking software Kinovea.

Kinematic analysis during open phase

Angular velocities of mandible movements during open phase were measured using high-speed images. The tip of both sides of mandibles was filmed at 1000 fps and

tracked to measure the angular velocity using the video tracking software Kinovea.

To analyze the latch kinematics of the open phase movements, we constructed statistical models to estimate the parameters using the probabilistic programming language Stan through the R package "rstan". We assumed the pivot point was stationary and estimated the point by fitting circles to the trajectories. The time series of the angular position were obtained. The instantaneous velocity was calculated using five-point stencil approximation:

$$f'(t) \approx \frac{-f(t+2h)+8f(t+h)-8f(t-h)+f(x-2h)}{12h}.$$

Our model for the angular velocity had the two components, (1) the whole value μ and (2) specific value to each strike μ_{strike}:

$$AngularVelocity[n] \sim Normal(\mu[n] + \mu_{strike}[StrikeID[n]], \sigma_w), n = 1, \ldots, N_{data}.$$

The μ at the current angular position was considered similar to the previous position, thus the μ is softly constrained by the normal distribution with a parameter σ_t:

$$\mu[2{:}\,N_{theta}] \sim Normal(\mu[1{:}\,N_{theta} - 1], \sigma_t).$$

The strike specific value can be generated from this distribution with the mean value specific to each individual animal μ_{animal} and the standard deviation σ_1:

$$\mu_{strike}[s] \sim Normal(\mu_{animal}[StrikeToAnimal[s]], \sigma_1), s = 1, \ldots, N_{strike}.$$

The μ_{animal} assumed to be generated the Gaussian distribution with the mean 0 and the parameter σ_0:

$$\mu_{aimal}[a] \sim Normal(0, \sigma_0), a = 1, \ldots, N_{animal}.$$

X-ray micro-computed tomography imaging

The trap-jaw ants *O. kuroiwae* were anesthetized using carbon dioxide and were fixed with alcoholic Bouin's fixative in a refrigerator (3□) for 2 days. After fixation, samples were dehydrated with ethanol series (70% twice, 80%, 90% and 100% for 60 min each). They were stained using 1% iodine diluted in dehydrated ethanol for 2 days. The staining enhances contrast of each ant tissue when X-ray micro-computed tomography (micro-CT) scan was performed. After samples were stained, they were transferred to liquidized *t*-butyl alcohol. The melting point of *t*-butyl alcohol is 25.5°C and liquidized t-butyl alcohol obtained by warming at 40□ was used. Samples were then placed in a refrigerator (3°C) to freeze *t*-butyl alcohol quickly. They were then freeze-dried by using a handmade freeze dry system that is composed from a vacuum evaporator (PX-52, Yamato Ltd., Japan) with a cold alcohol trap (H2SO5, AS ONE, Japan). All chemicals were obtained from Kanto Chemical Co. (Tokyo, Japan).

Samples were scanned on an X-ray micro-CT system (inspeXio SMX-100CT, Shimadzu Corporation, Kyoto, Japan) whose X-ray source was operated at 40 kV and 100 μA. The images were reconstructed with a voxel size of 2-3 μm. Image reconstruction and rendering were carried out using software VGStudio MAX (ver. 2.2.6 125, Volume Graphics, Heidelberg, Germany) and amira (ver. 2019.1, Thermo Scientific, Waltham, USA). Some of the CT images were converted into STL files to print out 3D models using a 3D printer (REPLICATOR2, Makerbot, New York, U.S.A.). The 3D models were magnified 110 times and used to examine the movement of the mandible joint.

X-ray *in vivo* live imaging

The X-ray *in vivo* live imaging was performed using the synchrotron at SPring-8 in Hyogo Japan. The trap-jaw ant *O. kuroiwae* were scanned in Hutch 3 of beamline 20B2, located over 200m from the storage ring whose X-ray source was operated at 33 keV. The ant was mounted on a plastic rod platform using the dental wax not to move the head during the experiment. It was placed between the X-ray source and the detector. The live images were recorded using Hamamatsu phosphor charge-coupled device (CCD) detector (C4742-95HR) with an active area of 24 × 15.7 mm^2 (100 fps). All images were recorded with a spatial resolution of approximately 2.74 μm. Beam inhomogeneities and detector artefacts were corrected with custom software using images of the direct beam and detector dark current. All images scanned were saved as TIFF format and reconstructed using image processing software Image J (NIH, ver 2.0.0).

Results

We here focused on the 3D structure of the mandible join to gain the understandings the latching mechanism of the trap-jaw ant *O. kuroiwae*. The morphology of *O. kuroiwae* was similar to that of *O. monticola*. The body color of these species is both brown, however the *O. monticola* is much darker than *O. kuroiwae*. The body mass of the *O. kuroiwae* is smaller than *O. monticola*. The matured workers of *O. kuroiwae* were 11.2 ± 1.13 mg (mean ± SD, N=10) and that of *O. monticola* was 14.6 ± 1.62 mg (N=8) (Table 1). The single mandible mass of the *O. kuroiwae* was 261 ± 3.51 μg (mean ± SD, n=20) and *O. monticola* was 360 ± 4.37 μg (n=16).

Mandible powered bouncer defense

Mandible powered jump was observed during predator-prey encounter (Sup. 1). To introduce the mandible powered jump, we used the tactile stimulus onto the mandible. Since most of the trap-jaw ants responded with dart escape behavior to the unexpected tactile stimulus (Aonuma, 2020), we analyzed the bouncer defense successfully recorded. Ballistic propulsion originated from the ultrafast movement of the mandible (Fig. 1A, B, Sup. 1). The maximum angular velocity of the mandible was (2.3 ± 0.7) $\times 10^4$ rad/s (N=5, n=46, mean ± SD) in *O. kuroiwae* and (1.4 ± 0.4) $\times 10^4$ rad/s (N=4, n=38, mean ± SD) in *O. monticola*. Although *O. kuroiwae* closed the mandible significantly faster than *O. monticola*, there was no significant difference in the velocity of the mandible powered jump between *O. kuroiwae* and *O. monticola* (Fig. 1C). The maximum velocity of the mandible powered jump in *O. kuroiwae* was 0.852 ± 0.327 m/sec (N=10, n=20, mean ± SD) and that in *O. monticola* was 1.042 ± 0.589 m/sec (N=8, n=24).

Latching the mandible

To power the mandible at an ultra-high speed, the trap-jaw ant utilizes the latching mechanism of the mandible joint. To unveil the anatomical structure of the latch embodied, we performed X-ray micro-imaging. X-ray micro-CT scanning allowed us to reveal the arrangement of mandibular muscles and the three-dimensional anatomical structure of the apodeme, endoskeleton, and exoskeleton of the ant (Fig. 2, Sup. 2). The movement of the mandible is expressed by the sequential movements: open, latch, load, and strike. At the open phase, contraction of the abductor muscles opened the mandible fully, and then the mandible was kept open until the adductor muscles contracted to close it. The adductor muscles contributed to close the mandible at both a

slow speed and an ultra-high speed. The loading phase driven by a strong contraction of adductor muscles is necessary to power the mandible at an ultra-high speed.

To observe the adductor muscles during the open phase, we CT-scanned the ant with the right mandible opened and the left mandible closed. When the right mandible was fully opened, the adductor muscles were extended (Fig. 2, Sup. 2). The extension of the adductor muscles was caused by the contraction of the abductor muscles. The contraction of the abductor muscles rotates the mandible to open, which pulls the apodeme to extend the adductor muscles (Fig. 2A, B). The angle between the muscle fibers and the apodeme on the right side was narrow. On the other hand, the left abductor muscles were more contracted than the right-side abductor muscles. The micro-CT scanning allowed us to observe the trigger muscles (Fig.2 B). The trigger muscle is thought to contribute to releasing the latched mandible to power at an ultra-high speed (Gronenberg, 1995). The contraction of the abductor muscle also extended the trigger muscles. The angle of the trigger muscles was slightly changed when the mandible was fully opened. The rotation of the mandible joint also moved the endoskeleton that connects to the apodeme of the mandible. These movements were also observed using synchrotron live imaging (Fig. 3, Sup. 3). The apodeme attaching to the adductor muscles was pulled with slightly twisting during the open phase that is caused by the contraction of the abductor muscles (Fig.3 B). The position of the apodeme twisted was kept until the contraction of the adductor muscle occurred to close the mandible. During the loading phase, the apodeme was twisted back to the almost original position (Fig. 2C). At the loading phase, strong contraction of the adductor muscles made the exoskeleton of the head deformed (Sup. 3). The strike phase is caused by the release of the latching mandible. At the strike phase, the

apodeme of the mandible slightly moved to the original position where the adductor muscles were relaxed (Fig. 3D). The exoskeleton deformed by the muscle contraction was also recovered to the original shape.

The *in vivo* X-ray live imaging demonstrated that the structure of the mandible joint was a ball-socket like joint (Fig. 4). The bulge at the jaw acts as a ball to rotate into the socket when the mandible opened. To identify the anatomical structure of the latch at the mandible joint, X-ray micro-CT images were then reconstructed (Fig. 5). The micro-CT scanning revealed that there was a U-shaped rail-like structure on the ventral surface of the lip at the socket part of the joint (Fig. 5A-2 double asterisk, Sup. 2 and 4). At the ventral side of the ball, there was a protuberance that did not slide into the socket when the mandible opened but slid on the rail (Fig. 5A-2 asterisk). To examine how the protuberance slide on the rail, the mandible joint was reconstructed using a 3D printer (Fig. 6, Sup. 4-6). The 3D model well reproduces the anatomical structure. The 3D model demonstrated that there is a projection just before the terminal of the rail (Fig. 6B). The protuberance slid on the rail of the socket and the tip of the protuberance could get over the ridge of the projection to terminate at the groove like structure.

Micro-CT scanning revealed that the ball of the mandible has another detent ridge. On the surface of the ball lip, a fine projection was observed (Fig. 5A-1, 2, arrow). The height of the detent ridge was 3.8 ± 1.8 μm (N=7, n=12, mean ± SD). This part was slid into the socket of the joint when the mandible opened (Fig. 4). Micro-CT scanning also revealed that there was other projection on the surface of the inner section of the socket. The height of the detent ridge on the surface of the cuticular at the socket was 6.8 ± 2.7 μm (N=7, n=12, mean ± SD). These anatomical structures of the mandible

ball joint suggested to us that the ball that has a detent ridge slides into the socket and over the ridge of the socket followed by snapping back at the edge of the groove. If so, the angular velocity of the mandible during the open phase must change when snapping back at the edge of the groove.

Latching kinematics

To quantitatively confirm the functional aspect of the projection on the surface of the detent ball corresponding to the groove at the end of the socket, we examined the change in the angular velocity of the mandible during the open phase (Fig. 6). The movements of the tip of the mandible were tracked and analyzed (N=10, n=42). The latching kinematics demonstrated that the angular velocity of the mandible increased just before the position fully opened. The peak in the angular velocity occurred about 10 degrees before the final position of the mandible. This movement indicated that the mandible was lured into the final stable position. The blue line marks in the Figure 6 estimated angular velocity as a function of angular position of the mandible based on the statistical model (see materials and methods). We built two statistical models to examine the kinematic difference between the two species *O. kuroiwae* and *O. monticola*, but almost the same kinematic changes were obtained. Variations among the trials and individuals were larger than those of species. Since the anatomical structure of the ball joint of the two species were also quite similar, we here show the result estimated on the statistical model combining the two species.

Discussion

The trap-jaw ants strike the mandible at an ultra-high speed when hunting (De la Mora et al., 2008) and mandible powered jumping (Larabee and Suarez, 2015). The genus *Odontomachus* has supplied us with a good model system to investigate the mechanisms underlying the ultra-fast movement of the appendage (Gronenberg et al., 1993; Larabee and Suarez, 2015; Sutton et al., 2022; Wang et al., 2020). The maximum angular velocities of the mandible have been reported in some *Odontomachus* species (Spagna et al., 2008; Spagna et al., 2009; Larabee et al., 2017). Here, we gained information about other two species, *O. kuroiwae* and *O. monticola*. Although the maximum angular velocity of *O. kuroiwae* was faster than *O. monticola*, the velocity of the bouncer defense was similar. Since the body mass of *O. kuroiwae* was smaller than that of *O. monticola*, *O. kuroiwae* might be more influenced by the viscosity of the air during the jump than *O. monticola*. To understand the difference in the velocity between the two species, measuring strike force of the mandible and kinematic analysis of the mandible powered jump is necessary as a next step.

Prior to the mandible strike, the trap-jaw ant loads elastic energy and amplifies the power to produce ultra-fast movement (Patek et al., 2006; Sutton et al., 2022). During loading, strong contraction of the mandible adductor muscles pulled the mandibular apodemes and deformed the exoskeleton of the head. The elastic deformation of the apodeme and skeleton function as a spring to store the energy for the power of striking.

The spring and latch systems including synthetic systems are diverse and operate under their own mass-specific power limits (Ilton et al., 2018). In the locust, semi-lunar process (SLP) at the femur-tibia joint is bent to store energy for use during kicking and jumping (Cofer et al., 2010). To release the amplified power to produce

extremely fast movement, the catapult mechanism is thought to be the key in invertebrate, for example, locust: (Wan et al., 2016), click beetle: (Bolmin et al., 2019), snapping shrimp: (Ritzmann, 1973; Ritzmann, 1974; Kaji et al., 2018), mantis shrimp: (Patek et al., 2004; Patek et al., 2007; Zack et al., 2009) The catapult mechanism is also thought to contribute to producing quick movement in vertebrates, like frog jump (Astley and Roberts, 2012; Astley and Roberts, 2014). To utilize the catapult mechanisms, arthropods embodied diverse latch mechanisms to lock strike bodies in place during building up elastic energy to be released as kinetic energy of their strike bodies (Ilton et al., 2018).

Releasing a latch allows the joint to move extremely fast via recoil. The mechanisms underlying ultra-fast movements of the trap-jaw ants have been investigated and the latch mechanism to lock the joint has been demonstrated (Gronenberg, 1995). However, the detailed anatomical structure of the latch remained unclear. The X-ray live imaging and 3D model allowed us to observe the structure and the movement of the mandible joint. The contraction of the mandible abductor muscles opens the mandible. The joint of the mandible forms a ball joint and the rotation of the ball in the socket could make the mandible stable. The micro-CT scanning revealed another anatomical rail-like structure on the surface of the mandible socket. The U-shape rail structure was on the ventral surface of the lip of the socket part of the joint. This rail is held by the protuberance on the ventral side of the mandible ball (Sup. 4). When the mandible opens, the protuberance slides on the rail. The tip of the protuberance gets over the ridge of the projection to terminate at the groove like structure. The rail and protuberance consist of the hard cuticle and these anatomical structures would function to rotate the mandible stably open. The anatomical structure

consists of the protuberance tip and the projection which could function to catch the mandible fast. The hard cuticle of these structures could be a support for the ball, preventing it to slip into the socket during the loading phase and deform the elastic exoskeletal structure of the head. Therefore, these anatomical structures not only function as a part of the latch system but also function to support the stability of the mandible strike.

X-ray micro-CT scanning revealed another candidate of the anatomical structure forming a part of the latch system in the mandible joint. The ball of the mandible has a projection at the lip of the lateral area. When the jaw is opening, this area slides into the socket of the mandible joint. The socket also has a projection of a similar size. These anatomical structures can function as a detent ridge, i.e., the ball slides into the socket and the projection of the ball gets over the projection of the socket followed by snapping back at the edge of the groove. The kinematic analysis demonstrated that the angular velocity of the mandible becomes faster just before terminating the movement at the open phase. Therefore, this detent ridge would also function as the latch mechanism.

Through the loading phase, strong contraction of the adductor muscles gradually frustrates the multiple spring and latch mechanisms, which induces deformation of the head exoskeleton by pulling the mandible apodeme. The state is into a minimally stable, critical point, which makes it sensitive and easy to release the latch by the trigger system. The trigger muscles are known to be activated just before the strike (Gronenberg, 1995). Contraction of the trigger muscle applies lateral force to the apodeme, which initiates the mandible strike. Micro-CT scanning demonstrated that the trigger muscle changed the angle when abductor muscles contract to open the

mandible. Furthermore, the movement of the 3D model demonstrated that the trajectory of the opening mandible slightly twisted just before latching.

In sum, this study demonstrates that the mandible joint of the trap-jaw ant genus *Odontomachus* is a ball joint that has multiple latches forming a system consisting of the detent ridge structures on the surface of the ball. To further gain an understanding of the mechanisms to power the mandible at an ultra-high speed, it will be necessary to investigate how each mandible muscle work to store elastic energy in the spring system and to recoil the power. X-ray micro live imaging will allow us to investigate them in detail.

Table 1. Velocity of mandible powered jump of the trap-jaw ants.

	O. kuroiwae	*O. monticola*
Body mass (mean±SD)	11.2 ± 1.13mg (N=10)	14.6 ± 1.62mg (N=8)
Single mandible mass	261 ± 3.51μg (n=20)	360 ± 4.37μg (n=16)
Jump velocity	0.852 ± 0.327m/s (n=20) (N=10)	1.042 ± 0.589m/s (n=24) (N=8)

Acknowledgements

A part of this work was supported by JST CREST Grant Number JPMJCR14D5, and by Japan Society for the Promotion of Science KAKENHI [Grant-in-Aid for Scientific Research (A), grant number 22H00216, and Grant-in-Aid for Challenging Exploratory Research, grant number 22K19795], Japan. Synchrotron experiments were supported by JASRI (2018A1240 and 2018A1244). We thank Drs. K. Uesugi and H. Iwamoto at Spring-8 for their comments and technical support and Ms. Valeria Zeni at the University of Pissa for her comments on the manuscript.

Figure legends

Figure 1: (A) Mandible powered jump of the trap-jaw ant *O. kuroiwae*. The trap-jaw ant represented a defensive posture toward a potential threat. The ant opened the mandible widely before closing extremely fast to strike an obstacle (handle of the forceps). The reaction force of the strike made the ant jump. It took within 0.4 msec to close the mandible from the fully opened position to the closed position. The behavior was recorded by a high-speed camera and the recording frame rate was 10,000 fps. (B) Angular velocity of the mandibles during ultra-fast movements of the 2 species *Odontomachus kuroiwae* (n=46) and *Odontomachus monticola* (n=38). The angular velocity of the mandible in the *O. kuroiwae* was significantly fast than that in the *O. monticola* ($p < 0.0001$, Mann-Whitney test). Each dot plotted indicates the value of each trial. The bar indicates the median. (C) The maximum angular velocity of the mandible. The jump speed of both species was not significantly different (Mann-Whitney test). Each dot plotted indicates the mass of the single side of the mandible. The bar indicates the median.

Figure 2: Reconstruction of the X-ray micro-CT imaging of the trap-jaw ant. (A) Dorsal view of the head that was reconstructed at a different focal plane by using a software VGstudio Max Ver 2.2. (B) Segmentation images of the adductor and abductor muscle by using software amira 3D Ver.2021.1. Abd: abductor muscles, Add: adductor muscles, Apd: apodeme, Br: brain, Ensk: endoskeleton, SoG: suboesophageal ganglion, Trm: trigger muscle.

Figure 3: X-ray imaging of the head of the alive trap-jaw ant (Sup. 2). (A) Relaxed the

position of the mandible. (B) At the end of the open phase, the mandible is fully opened and latched. The apodeme that connects to the adductor muscle twitched. (C) Loading phase. The exoskeleton was deformed by the strong contraction of the adductor muscles. The adductor apodeme twitched back nearly to the original position. (D) Strike phase. Just after the strike, the deformed exoskeleton of the head recovered to its original shape. The apodeme did not move much.

Figure 4: X-ray live imaging of the head of the alive trap-jaw ant (Sup. 2). (A) Reconstruction of the mandible of the trap-jaw ant. The left side is the dorsal view, and the right side is the ventral view of the mandible. (B) Snapshots of the X-ray live imaging during the open phase (0 - 0.75 sec), loading phase (1.1 sec), and the strike phase (1.2 sec).

Figure 5: (A) Reconstructed images of the mandible joint (Sup. 3). A-1: dorsal view of the mandible joint. A-2: Ventral view of the framed area indicated in the A-1. The arrow shows the projection of the ball part of the mandible joint. The single asterisk indicated the protrude at the ball part of the mandible. Double asterisks indicate the rail-like structure of the ridge of the socket part of the mandible joint. A-3: Inside of the socket part of the mandible joint. The arrow indicates the projection on the surface of the exoskeleton. (B)The height of the projection on the surface of the mandible joint. Box-and-whisker graphs indicate minimum, median, maximum, and 25th and 75th percentiles.

Figure 6: 3D model of the mandible joint (Sup. 4). (A) Socket and ball of the

mandible joint were separately printed out using a 3D printer. (B) The ball of the joint was placed in the socket and moved. From B-1 to B3 are snapshots of the different angles of the joint. Right-side images are the rail system of the mandible that is framed in the area indicated in the left-side images. The single asterisk indicated the protrude at the ball part of the mandible. Double asterisks indicate the rail-like structure of the ridge of the socket part of the mandible joint. Arrow indicates another projection where the protrude of the ball is terminated.

Figure 7: Latching kinematics revealed the increase of opening velocity just before the latched position. (A) The ants open the mandible and the velocity of the movement shows the peak about 10 degrees before the final position of the mandible, revealing that the mandible is lured into the final stable position. The blue line marks the estimated angular velocity as a function of the angular position of the mandible based on the statistical model (see materials and methods). (B) Change of the opening velocity for each individual and species. It largely varied within and across individuals, but no difference between species.

Supplementary

Sup. 1: Highspeed movie of mandible powered jump captured at 10,000 fps.

Sup. 2: X-ray live imaging during the ultra-fast movement of the mandible of the trap-jaw ant.

Sup. 3: Movie of the X-ray micro-CT images of the trap-jaw ant.

Sup. 4: 3D model of the mandible joint. Digital data of the micro-CT images were converted into STL files and then printed out using a 3D printer. The movie was made using a series of snapshot of the 3D model with different positions of the mandible.

Sup. 5: STL file of the socket of the mandible joint used to make a 3D model.

Sup. 6: STL file of the ball of the mandible joint used to make a 3D model.

References

Aonuma, H. (2020). Serotonergic control in initiating defensive responses to unexpected tactile stimuli in the trap-jaw ant *Odontomachus kuroiwae*. *J. Exp. Biol.* **233**.

Astley, H. C. and Roberts, T. J. (2012). Evidence for a vertebrate catapult: elastic energy storage in the plantaris tendon during frog jumping. *Biol. Lett.* **8**, 386-389.

Astley, H. C. and Roberts, T. J. (2014). The mechanics of elastic loading and recoil in anuran jumping. *J. Exp. Biol.* **217**, 4372-8.

Bolmin, O., Wei, L., Hazel, A. M., Dunn, A. C., Wissa, A. and Alleyne, M. (2019). Latching of the click beetle (Coleoptera: Elateridae) thoracic hinge enabled by the morphology and mechanics of conformal structures. *J. Exp. Biol.* **222**, jeb196683.

Burrows, M. (1995). Motor patterns during kicking movements in the locust. *J. Comp. Physiol. A* **176**, 289-305.

Cofer, D., Cymbalyuk, G., Heitler, W. and Edwards, D. H. (2010). Neuromechanical simulation of the locust jump. *J. Exp. Biol.* **213**, 1060-1068.

De la Mora, A., Pérez-Lachaud, G. and Lachaud, J.-P. (2008). Mandible strike: the lethal weapon of *Odontomachus opaciventris* against small prey. *Behav. Proc.* **78**, 64-75.

Gronenberg, W. (1995). The fast mandible strike in the trap-jaw ant *Odontomachus*. *J. Comp. Physiol. A* **176**, 399-408.

Gronenberg, W. (1996). Neuroethology of ants. *Naturwissenschaften* **83**, 15-27.

Gronenberg, W. and Ehmer, B. (1996). The mandible mechanism of the ant genus *Anochetus* (Hymenoptera, Formicidae) and the possible evolution of trap-jaws. *Zool.* **99**, 153-162.

Gronenberg, W. and Tautz, J. (1994). The sensory basis for the trap-jaw mechanism in the ant *Odontomachus bauri*. *J. Comp. Physiol. A* **174**, 49-60.

Gronenberg, W., Tautz, J. and Holldobler, B. (1993). Fast trap jaws and giant neurons in the ant odontomachus. *Science* **262**, 561-3.

Heitler, W. (1974). The locust jump. *J. Comp. Physiol.* **89**, 93-104.

Ilton, M., Bhamla, M. S., Ma, X., Cox, S. M., Fitchett, L. L., Kim, Y., Koh, J. S., Krishnamurthy, D., Kuo, C. Y., Temel, F. Z. et al. (2018). The principles of cascading power limits in small, fast biological and engineered systems. *Science* **360**. 6387.

Just, S. and Gronenberg, W. (1999). The control of mandible movements in the ant *Odontomachus*. *J. Insect Physiol.* **45**, 231-240.

Kaji, T., Anker, A., Wirkner, C. S. and Palmer, A. R. (2018). Parallel saltational evolution of ultrafast movements in snapping shrimp claws. *Curr. Biol.* **28**, 106-113. e4.

Larabee, F. J., Gronenberg, W. and Suarez, A. V. (2017). Performance, morphology and control of power-amplified mandibles in the trap-jaw ant *Myrmoteras* (Hymenoptera: Formicidae). *J. Exp. Biol.* **220**, 3062-3071.

Larabee, F. J. and Suarez, A. V. (2015). Mandible-powered escape jumps in trap-jaw ants increase survival rates during predator-prey encounters. *PLoS ONE* **10**, e0124871.

Patek, S., Baio, J., Fisher, B. and Suarez, A. (2006). Multifunctionality and mechanical origins: ballistic jaw propulsion in trap-jaw ants. *PNAS* **103**, 12787-12792.

Patek, S. N., Korff, W. and Caldwell, R. L. (2004). Deadly strike mechanism of a mantis shrimp. *Nature* **428**, 819-820.

Patek, S. N., Nowroozi, B., Baio, J., Caldwell, R. L. and Summers, A. P. (2007). Linkage mechanics and power amplification of the mantis shrimp's strike. *J Exp Biol* **210**, 3677-3688.

Pritchard, G. (1965). Prey capture by dragonfly larvae (Odonata; Anisoptera). *Canad. J. Zool.* **43**, 271-289.

Ritzmann, R. (1973). Snapping behavior of the shrimp Alpheus californiensis. *Science* **181**, 459-460.

Ritzmann, R. E. (1974). Mechanisms for the snapping behavior of two alpheid shrimp, *Alpheus californiensis* and *Alpheus heterochelis*. *J. Comp. Physiol.* **95**, 217-236.

Spagna, J. C., Schelkopf, A., Carrillo, T. and Suarez, A. V. (2009). Evidence of behavioral co-option from context-dependent variation in mandible use in trap-jaw ants (*Odontomachus* spp.). *Naturwissenschaften* **96**, 243-50.

Spagna, J. C., Vakis, A. I., Schmidt, C. A., Patek, S. N., Zhang, X., Tsutsui, N. D. and Suarez, A. V. (2008). Phylogeny, scaling, and the generation of extreme forces in trap-jaw ants. *J. Exp. Biol.* **211**, 2358-68.

Sutton, G. P., St Pierre, R., Kuo, C. Y., Summers, A. P., Bergbreiter, S., Cox, S. and Patek, S. N. (2022). Dual spring force couples yield multifunctionality and ultrafast, precision rotation in tiny biomechanical systems. *J. Exp. Biol.* **225** (14): jeb244077.

Tanaka, Y. and Hisada, M. (1980). The hydraulic mechanism of the predatory strike in dragonfly larvae. *J. Exp. Biol.* **88**, 1-20.

Versluis, M., Schmitz, B., von der Heydt, A. and Lohse, D. (2000). How snapping shrimp snap: through cavitating bubbles. *Science* **289**, 2114-2117.

Wan, C., Hao, Z. and Feng, X. (2016). Structures, properties, and energy-storage mechanisms of the semi-lunar process cuticles in locusts. *Sci. Rep.* **6**, 35219.

Wang, Z., Zhang, W., Wu, J. and Yang, Y. (2020). An approach to observing and quantifying real-time mandibular muscle topology in the trap-jaw ant *Odontomachus monticola* by synchrotron imaging. *J. Insect Behav.* **33,** 174-183

Yoshimura, M., Onoyama, K. and Ogata, K. (2007). The Ants of the Genus *Odontomachus* (Insecta: Hymenoptera: Formicidae) in Japan. *Species Diversity* **12**, 89-112.

Zack, T. I., Claverie, T. and Patek, S. N. (2009). Elastic energy storage in the mantis shrimp's fast predatory strike. *J. Exp. Biol*. **212**, 4002-9.

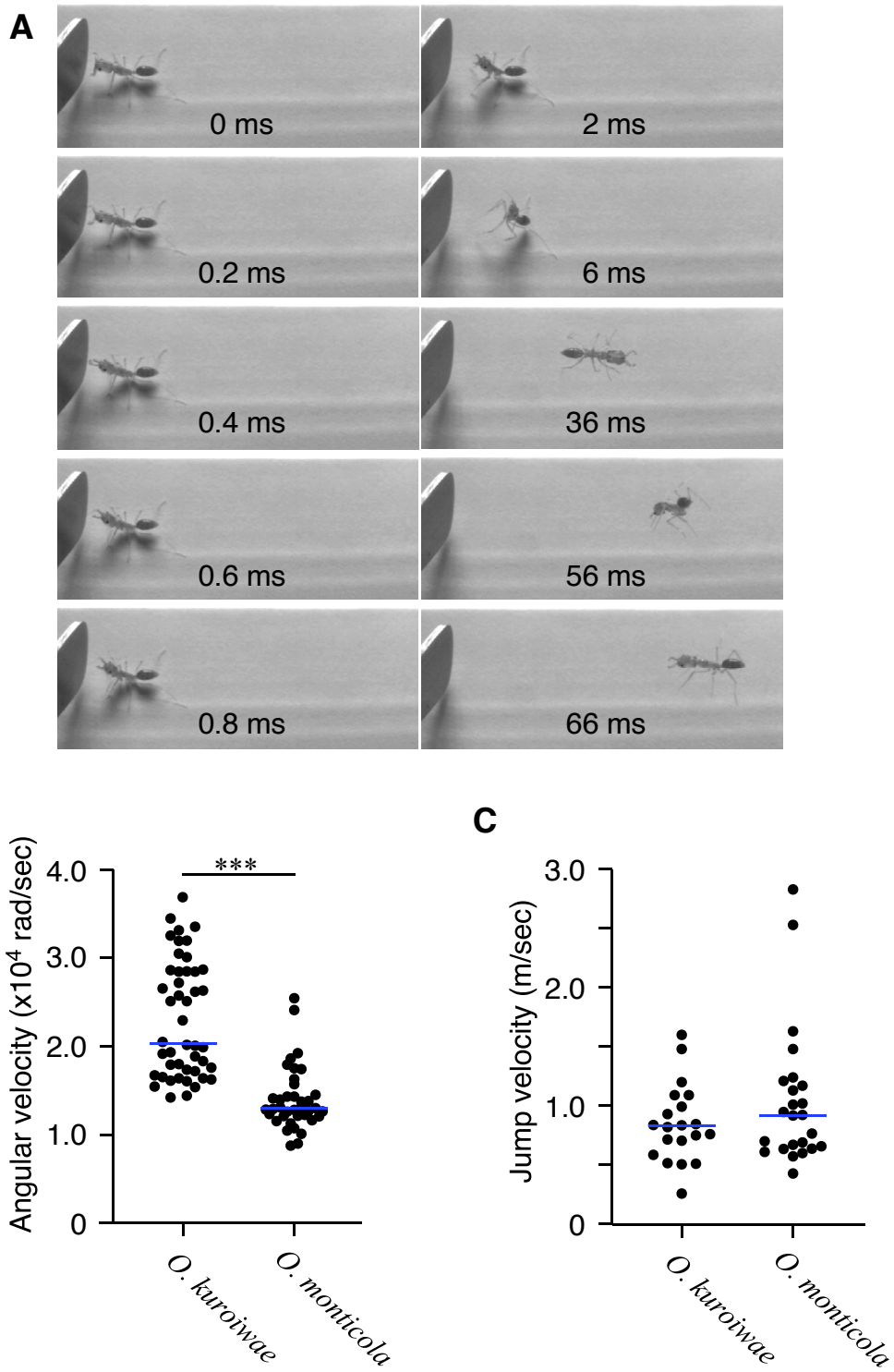
A
0 ms
2 ms
0.2 ms
6 ms
0.4 ms
36 ms
0.6 ms
56 ms
0.8 ms
66 ms
B
Angular velocity (x10^4 rad/sec)
4.0
3.0
2.0
1.0
0
***
O. kuroiwae
O. monticola
C
Jump velocity (m/sec)
3.0
2.0
1.0
0
O. kuroiwae
O. monticola

A

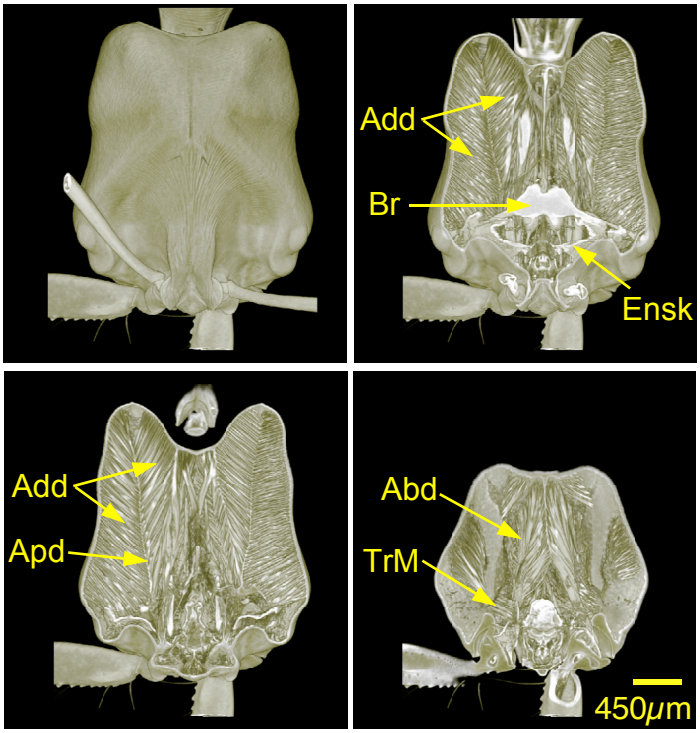
Add
Br
Ensk
Add
Apd
Abd
TrM
450μm

B

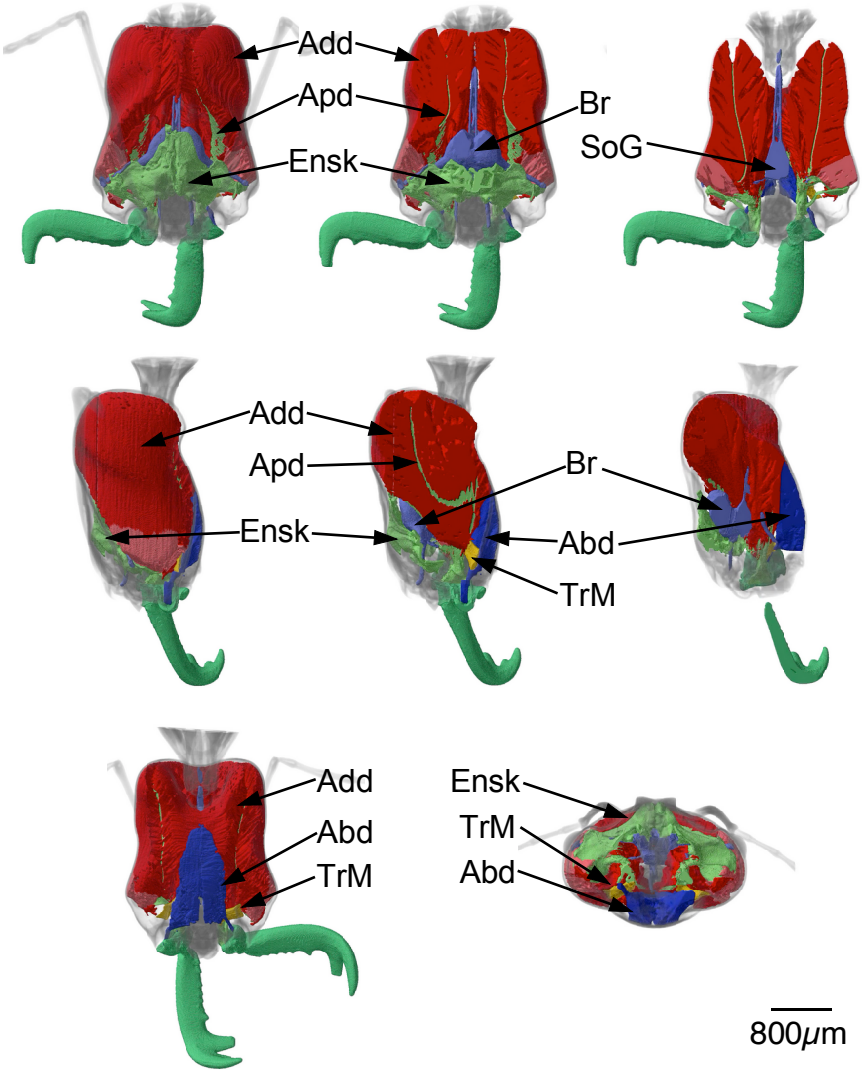
Add
Apd
Ensk
Br
SoG
Add
Apd
Ensk
Br
Abd
TrM
Add
Abd
TrM
Ensk
TrM
Abd
800μm

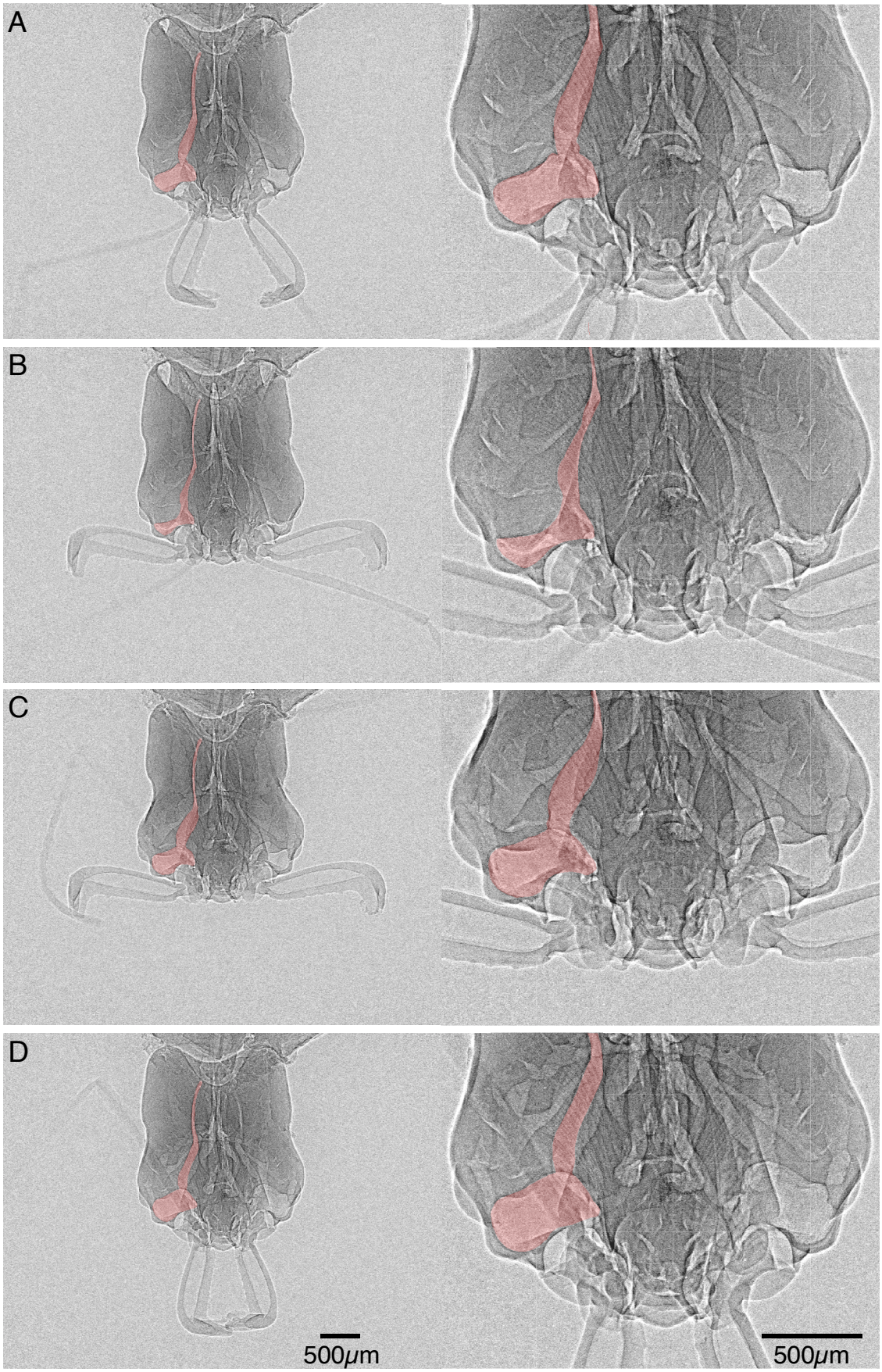
A
B
C
D
500μm
500μm

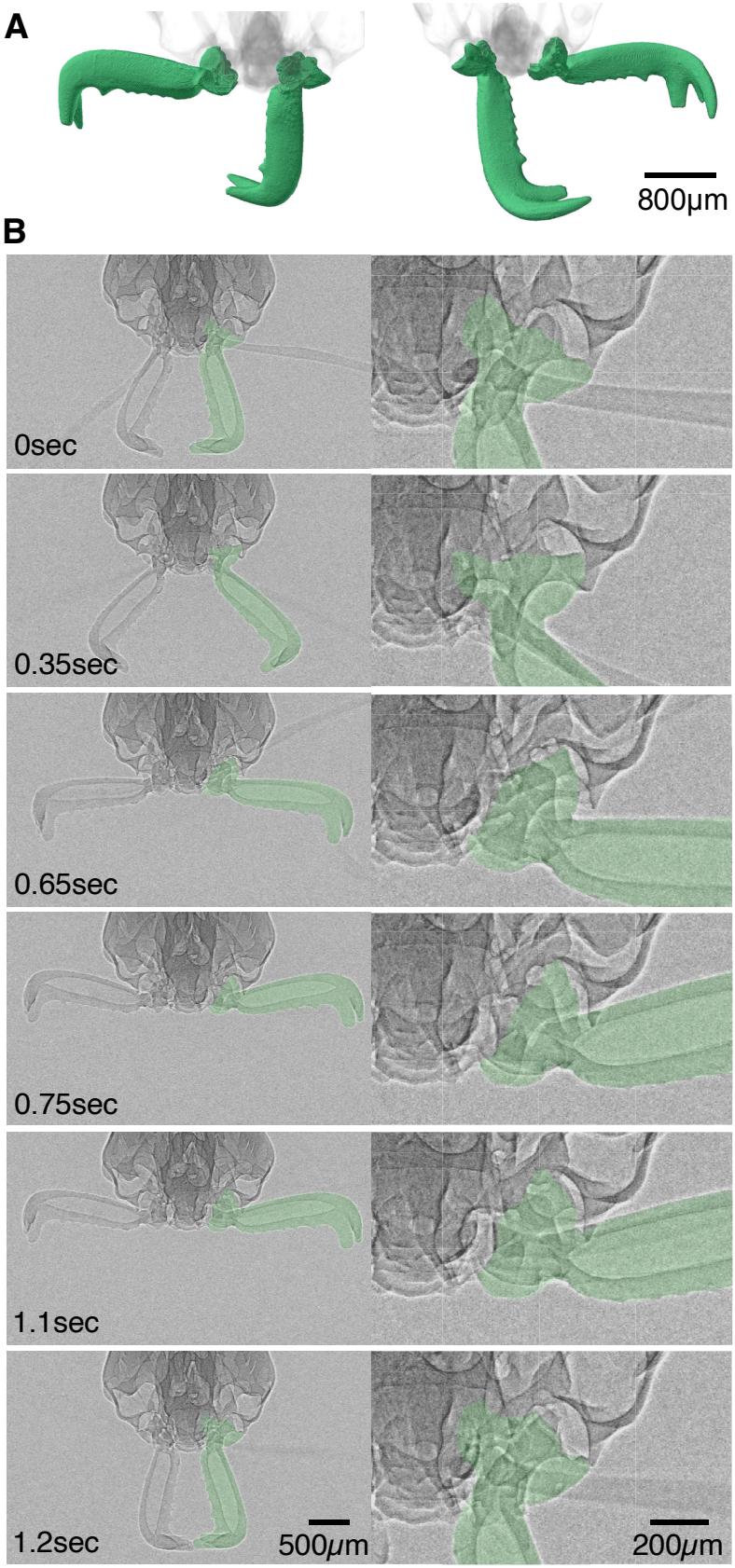
A
800μm
B
0sec
0.35sec
0.65sec
0.75sec
1.1sec
1.2sec
500μm
200μm

A-1

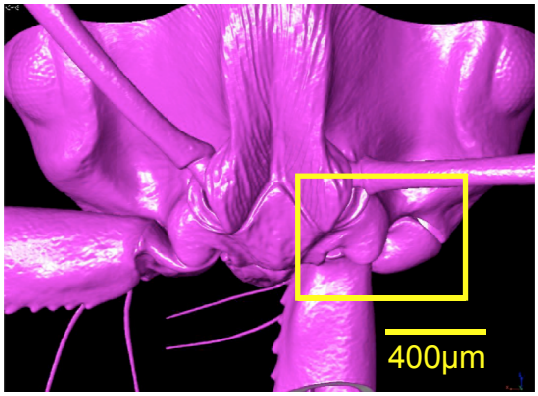
400μm

A-2

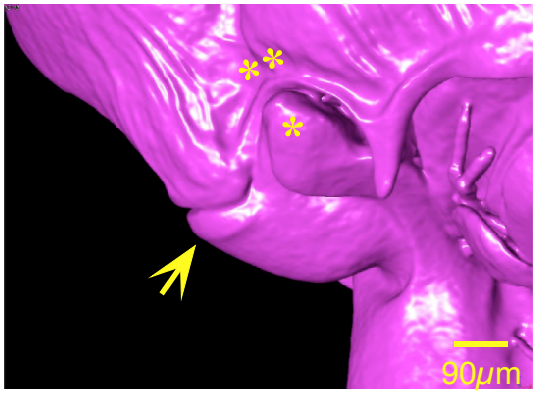
90μm

A-3

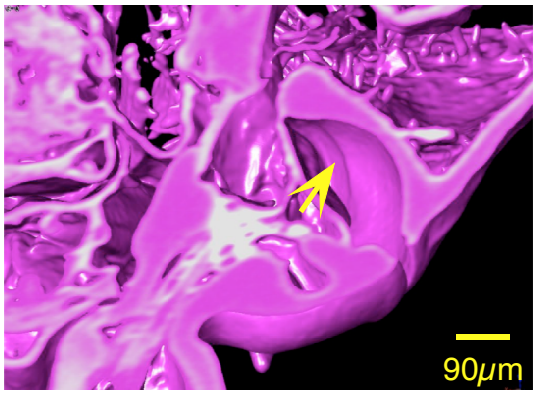
90μm

B

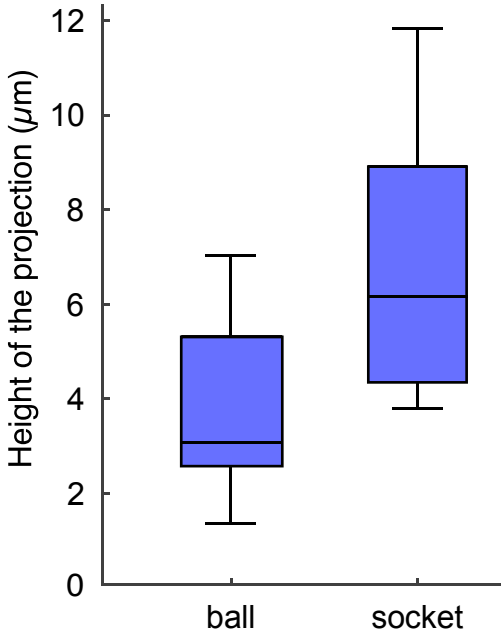
Height of the projection (μm)
0
2
4
6
8
10
12
ball
socket

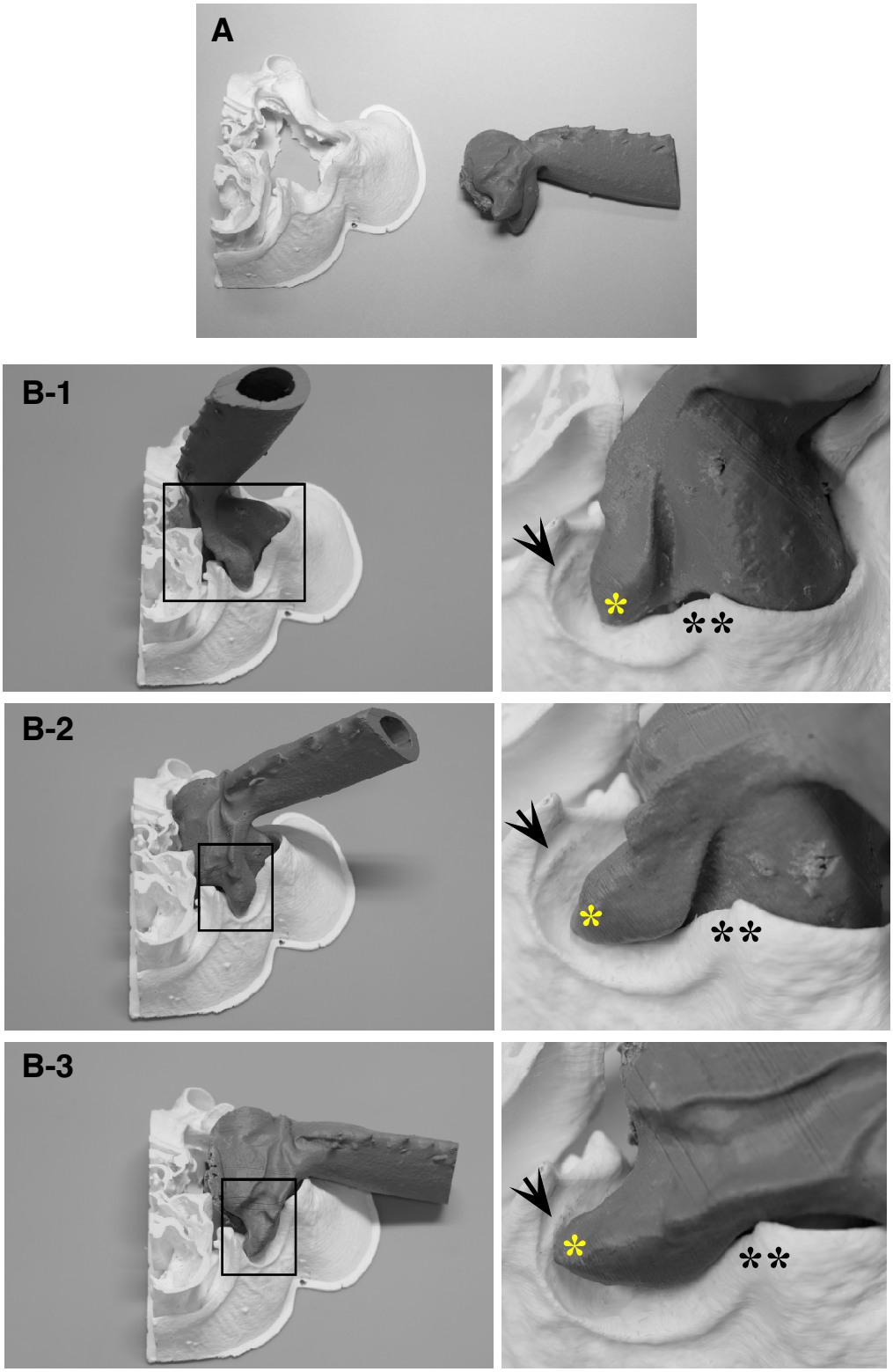
A
B-1
B-2
B-3

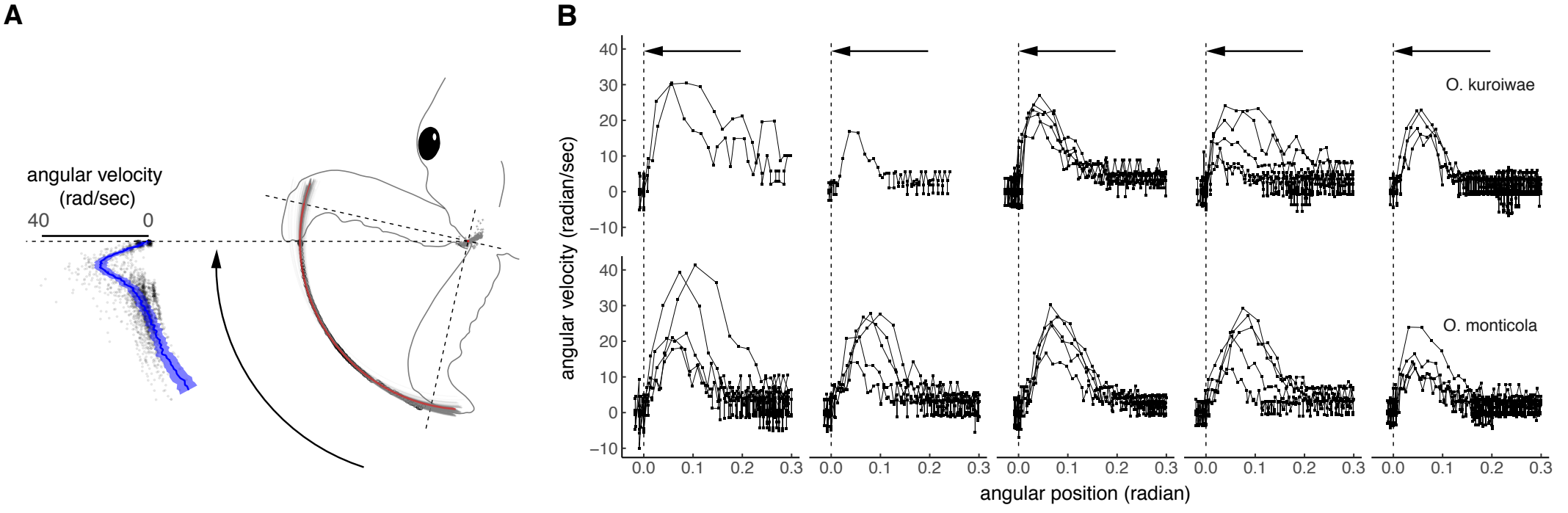
A
angular velocity
(rad/sec)
40
0
B
O. kuroiwae
O. monticola
angular velocity (radian/sec)
angular position (radian)
40
30
20
10
0
−10
0.0
0.1
0.2
0.3